Chapter 2
Background

Abstract The information necessary to support the model development and the literature to back the various discussions in the book is presented here. This chapter presents information on the different organic solvents and their properties, membrane materials and mechanical properties as well as the necessary membrane terminologies, and information on the model that provided insight into developing the model developed in this book.

Keywords Organic solvents · Membranes · Membrane performance · Membrane polymers · Membrane models · Membrane swelling · Membrane compaction · Young's modulus · Solubility parameter · Poisson ratio · Membrane rejection · Solvent-resistant · Membrane characterization · Solute distribution · Stress · Strain

2.1 Organic Solvents

Applications involving organic solvents is on the rise with a 2013 annual sales of 25 billion USD. Moreover, experts predict a 4 % rise in annual sales until 2021 [1]. Generally, organic solvents are grouped into polar and nonpolar solvents. Polar solvents are subcategorized into polar parotic and polar aprotic (Fig. 2.1 and Table 2.1). Table 2.1 presents examples of nonpolar, polar parotic, and polar aprotic solvents. Nonpolar solvents include toluene, hexane, and benzene [1]. Polar parotic have hydrogen atom attached to an electronegative atom such as oxygen and include water, ethanol, and acetic acid. Polar aprotic solvents have large dipole moments and dielectric constants compared with nonpolar solvents. They are very aggressive with their molecules having bonds that include multiple and large bond dipole. These multiple bond exists between carbon (C), nitrogen (N), sulfur (S), phosphorus (P), or oxygen, such as in ketones, aldehydes, ethyl acetate, and dimethylformamide (DMF) [2].

A. Anim-Mensah and R. Govind, *Prediction of Polymeric Membrane Separation and Purification Performances*, SpringerBriefs in Molecular Science,
DOI 10.1007/978-3-319-12409-4_2

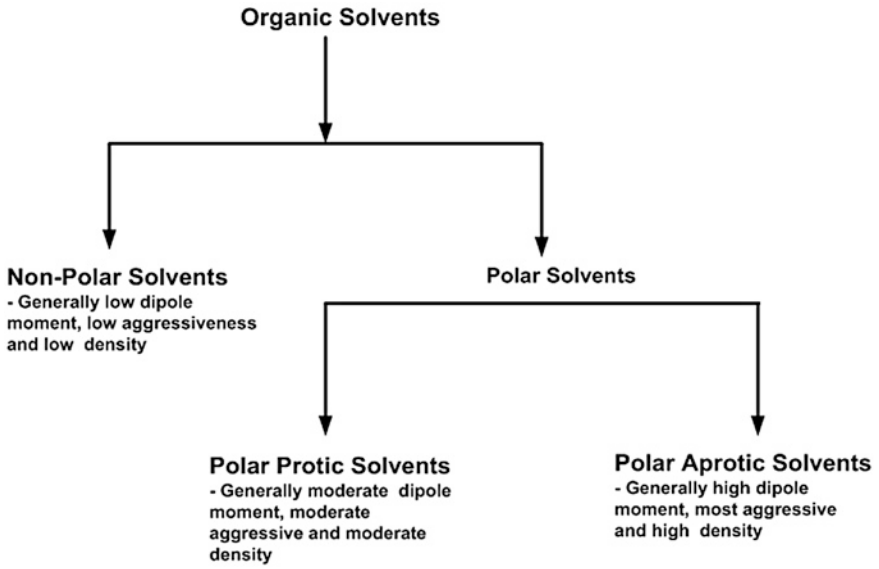

Fig. 2.1 General grouping of organic solvents [2]

Table 2.1 Properties of some organic solvents [3–5]

Solvents	Dielectric constant	Density (g/ml)	Dipole moment (D)	Solubility parameter ($MPa^{1/2}$)
Nonpolar solvents				
Pentane	1.84	0.626	0.00	14.5
Cyclopentane	1.97	0.751	0.00	16.6
Hexane	1.88	0.655	0.00	14.9
Cyclohexane	2.02	0.779	0.00	16.8
Benzene	2.30	0.879	0.00	18.8
Toluene	2.38	0.867	0.36	18.2
1,4 dioxane	2.30	1.033	0.45	20.7
Chloroform	4.81	1.498	1.04	18.8
Diethyl ether	4.30	0.713	1.15	15.1
Polar protic solvents				
Formic acid	58	1.210	1.41	24.9
n-Butanol	18	0.810	1.63	23.1
Isopropanol	18	0.785	1.66	24.9
n-Propanol	20	0.803	1.68	24.5
Ethanol	24.55	0.789	1.69	26.0
Methanol	33.00	0.791	1.70	29.7
Acetic acid	6.20	1.049	1.74	21.4
Water	80.00	1.000	1.85	47.9

(continued)

Table 2.1 (continued)

Solvents	Dielectric constant	Density (g/ml)	Dipole moment (D)	Solubility parameter ($MPa^{1/2}$)
Polar aprotic solvents				
Dichloromethane	9.1	1.327	1.60	20.0
Tetrahydrofuran	7.5	0.886	1.75	18.6
Ethyl acetate	6.02	0.894	1.78	18.2
Acetone	21	0.786	2.88	19.7
Dimethylformamide	38	0.944	3.82	24.8
Acetonitrile	37.5	0.786	3.92	24.7
Dimethyl sulfoxide	46.7	1.092	3.96	24.5
N-Methyl pyrrolidinone	32.2	1.028	4.1	22.9
Propylene carbonate	64	1.205	4.90	27.2

2.2 Some Membrane Performance Parameters and Models

For a membrane undergoing permeation, the various solute concentrations involved are the bulk solute concentration C_b, the permeate solute concentration C_{pi}, the membrane surface solute concentration C_s, and the solute concentration in the membrane C_m that are shown in the Fig. 2.2.

Note that C_m varies across the membrane thickness. For simplicity C_m at any point x along the membrane thickness can be calculated using $C_{mx} = C_s - (C_s - C_{pi})x/L$. For average solute concentration in the membrane, $x/L = 0.5$ could be used. C_m variation with the membrane thickness for each separation system is different so as the

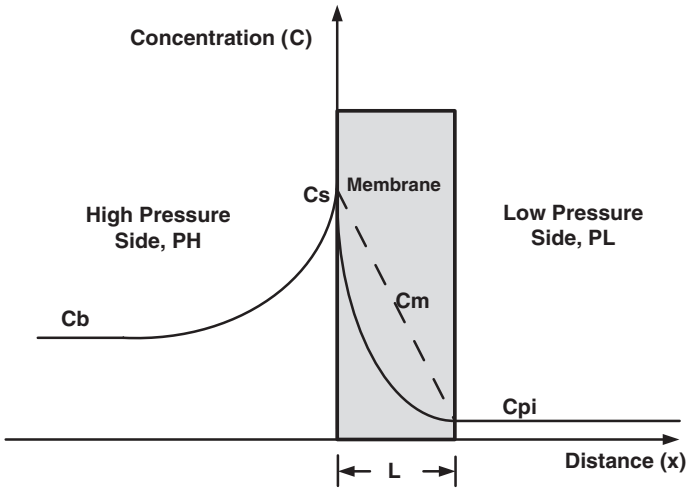

Fig. 2.2 Membrane under permeation solute concentrations

ratio of the C_{pi} to the C_m (i.e., $C_{pi}/C_m = K_d \leq 1$) at the various transmembrane pressures and feed rates. C_{pi}, C_s, and C_b are related to the flux q across the membrane, diffusivity D, and the concentration polarization layer δ as shown in Eq. 2.1 [2, 6, 7].

$$\frac{\delta}{D}q = \ln\left(\frac{C_s - C_{pi}}{C_b - C_{pi}}\right) \tag{2.1}$$

δ/D in Eq. 2.1 is obtained from Eq. 2.2 by knowledge of flux, transmembrane pressure ΔP, osmotic coefficient φ_m, solute concentrations in the bulk feed C_b and permeate C_{pi}, molar gas constant R, and temperature T. The hydraulic permeability L_p and the reflection coefficient σ^1 are also obtained by fitting Eq. 2.2 to experimental data [7, 8].

$$\ln\left[\frac{\Delta P - \frac{q}{L_p}}{\varphi_m RT\left(C_b - C_p\right)}\right] = \ln y = \frac{\delta}{D}q + \ln\sigma^1 \tag{2.2}$$

The basic parameters used to describe membrane performances include flux (q) and observed rejection (R_i) of species i [9]. The observed rejection is defined in Eq. 2.3;

$$\text{Observed Rejection } (R_i) = \left(1 - \frac{C_{pi}}{C_b}\right) \times 100\,\% \tag{2.3}$$

Equation 2.3 shows that an increase in C_{pi} results in a decrease in the objection rejection, i.e., membrane performance. Another parameter of interest is intrinsic rejection (r_i) of species i defined to take into consideration the concentration polarization layer C_s on the high pressure side of the membrane is as in Eq. 2.4 [9].

$$\text{Intrinsic Rejection } (r_i) = \left(1 - \frac{C_{pi}}{C_s}\right) \times 100\,\% \tag{2.4}$$

where C_{pi}, C_b, and C_s are the permeate solute concentration, bulk feed solute concentration, and the solute concentration at the surface of the membrane at the high pressure side, respectively. For a membrane retaining solute effectively, C_s is far greater than C_b. Membrane flux (q) is defined as in Eq. 2.5 [9];

$$\text{Flux } (q) = \frac{\text{Volume of Permeate}}{\text{Membrane Area} \times \text{Time}} \tag{2.5}$$

2.3 Some Factors Affecting Membrane Performance

Factors affecting polymeric membrane performance in organic systems include concentration polarization [9], swelling [10], compaction [11], fouling [12], and affinity between the solvent, solute, and membrane. Swelling and compaction are known to have negative effects on performance; however, they have some positive effects. Concentration polarization and membrane surface fouling could create a thin resistance layer that could improve membrane rejection, however, at

the expense of flux reduction in some cases. Swelling of membrane polymer by a solvent may indicate closeness in the individual solubility parameters. Swelling results in flux increase; however, excessive swelling could lead to excessive compaction which may lead to lower flux [2]. In addition, excessive swelling could reduce membrane rejection. Moreover, compaction reduces the membrane thickness which reduces the diffusion path resulting in increased flux; however, the increase compaction could also lead to increased membrane resistance leading to flux drop. Mechanically, excessive membrane swelling could result in low Young's' modulus since the strain could be high at a low applied transmembrane pressure. Reasonable transmembrane pressure on a swollen membrane could lead to low membrane rejection but high flux [11] since the swollen membrane network could transport the solutes easily across the membrane. However, in some situation, very high transmembrane pressure on slightly swollen membrane could lead to increase rejection but low flux if the concentration polarization builds up quickly.

2.4 In-Situ Real-time Swelling and Compaction Measurement

Ultrasonic time domain reflectometry (UTDR) are among the technologies which could be used to measure membrane swelling as well as compaction while the membrane is permeated with the solvent or solutions of interest in real time [2, 13]. Details of UTDR are found elsewhere [2].

2.5 Description of Material Mechanical Properties

Some parameters used to describe polymer mechanical properties depending on the application include the Young's (tensile or compressive), bulk, shear, and flexural moduli, tensile or compressive strength, yield stress and tensile or compressive strain and failure, and Poisson ratio. Most mathematical models use some of the above parameters in constitutive equations for descriptions and predictions of mechanical systems [14]. Table 2.2 shows some solvent resistant membrane materials with their respective Poisson ratios, Young's moduli (tensile and compressive), and solubility parameters and densities. Note that the parameters in Table 2.2 were obtained when the materials surfaces were unconstrained and under tension or compression. For pressure-driven solution–diffusion membranes, the surfaces are generally constrained and compacted while permeated at a given transmembrane pressure (compressive stress) and feed rate.

Figure 2.3 shows a homogenous membrane with initial thickness L_D, compacted while permeated at a transmembrane pressure (High HP–Low pressures LP). Homogenous membranes are made of one material and have either a dense or porous structure.

Table 2.2 Mechanical and physicochemical properties of some candidate solvent resistant membrane polymers obtained under unconstrained conditions [16–25]

Solvents	Tensile Young's modulus (E) (MPa)	Compressive Young's modulus (E) (MPa)	Poisson ratio (ν)	Solubility parameters δ ($MPa^{1/2}$)	Density (kg/dm^3)
Polydimethylsiloxane (PDMS)	0.27–0.83	0.56–3.59	0.5	14.9–15.59	0.95–1.25
Poly(1-(trimethylsilyl)-1-propyne) (PTMSP)	630	–	–	–	0.964
Cellulose acetate	2,100–4,100	–	0.40	21.9–27.8	1.29–1.30
Polyimide	2,000–3,000	2,500–4,100	0.34–0.42	–	1.42
Polyester	200–400	2,737–2,848	0.12–0.35	–	1.00–1.42
Polyphenylsulfone (PPSU)	2,340–2,480	1,730–1,931	0.42	20	1.29
Poly(ether ether ketone) (PEEK)	2,700–12,000	3,450–4,140	–	21.2–22.6	1.23–1.50
Polysulfone (PS)	2,480–8,690	2,580–8,000	0.37–0.42	20	1.24
Polyamide	1,500–16,000	2,241–2,896	0.30–0.50	22.87–27.8	1.06–1.39
Polyacylonitrile (PAN)	5,200	–	–	31.5	1.18–1.38
Polyether ketone (PEK)	3,190	–	–	20	1.27–1.43
Polyarylene ether ketone	–	–	–	–	–
Polyether sulfone (PES)	2,600–6,760	2,680–7,720	0.41	22.9–23.12	1.37–1.60
Polyetherimide (PEI)	2,900–3,447	2,900–3,300	0.36	–	1.28
Polyphenylene sulfide (PPS)	3,200–14,000	2,965	–	–	1.30–1.64
Poly(amide–imide)	4,500–18,600	4000–9900	0.39–45	–	1.38–1.42

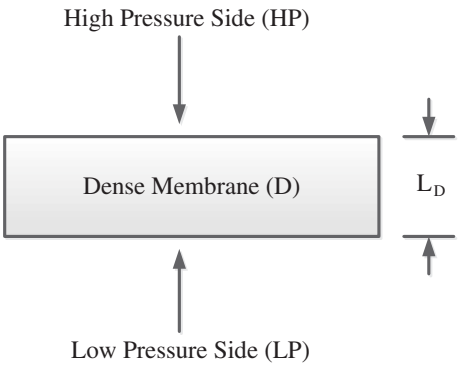

Fig. 2.3 A homogenous membrane under compression

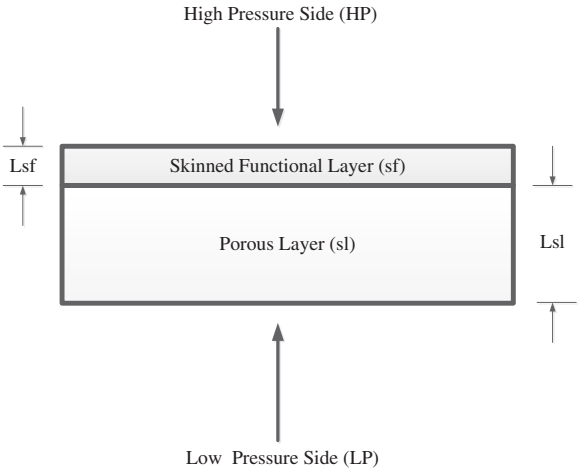

Fig. 2.4 An asymmetric with skinned functional layer membrane under compression

Figures 2.4 and 2.5 show asymmetric membranes with two (2) layers, i.e., a functional and support layers. Figure 2.4 shows an asymmetric membrane made of the same material but has a skinned functional layer (sf) and a support layer (sl); hence, different porosities or pore structures permeated at a transmembrane pressure.

Figure 2.5 shows an asymmetric membrane which the various layers, i.e., functional (f) and support layers (s) could be of different materials, hence different porosities or pore structures as in a composite membrane and permeated at a transmembrane pressure.

For a homogenous membrane (Fig. 2.3) under compression while permeated at a given transmembrane pressure same as compressive stress (σ), the compressive Young's modulus E_t is affected by the membrane material, porosity, and solvent–membrane interaction. The compressive Young's modulus E_t is obtained from the linear portion of the plot of the compressive stress (σ) or the transmembrane pressure versus the strain (ε) as shown in Eq. 2.6 [15];

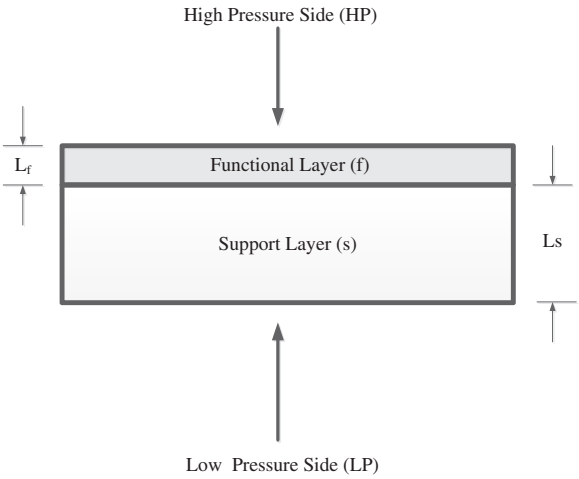

Fig. 2.5 An asymmetric with a functional layer membrane under compression

$$E_t = \frac{\text{Compressive Stress } (\sigma)}{\text{Strain } (\varepsilon)} \tag{2.6}$$

For an asymmetric membrane under compression while permeated at a given transmembrane pressure, each of the layers undergoes different strains. Let the stain for an asymmetric membrane with the functional layer (f) or the skin functional layer (sf) have with corresponding strains of ε_f while that of the support layer (s) or porous layer (sl) have a strain of ε_s. The individual compressive Young's modulus of each of the layers can be calculated as shown in Eq. 2.7 [15];

$$E_f = \frac{\sigma}{\varepsilon_f} \quad \text{and} \quad E_s = \frac{\sigma}{\varepsilon_s} \tag{2.7}$$

From knowledge of the individual compressive Young's modulus, the composite compressive Young's modulus can be calculated using Eq. 2.8 [15];

$$E_t = \frac{E_f E_s}{E_f L_f + E_s(1 - L_f)} \tag{2.8}$$

where $L_s\,(L_{sf}) + L_f\,(L_{sl}) = 1$ [15].

However, for a membrane made of layers undergoing permeation, it will be difficult to obtain the strain of the individual layers; hence, an overall strain will be necessary to obtain the composite compressive Young's modulus.

Most materials resist change in volume more than change in shape and are being defined by bulk and shear moduli, respectively. For most isotopic and elastic materials with unconstrained surfaces, the Poisson ratio (ν) is in the range of -1 to 0.5 (i.e., $-1 \leq \nu \leq 0.5$) for stability [26, 27]. However, situations including densification, anisotropism, and constrained surfaces could lead to material Poisson ratios out of the normal range ($-1 \leq \nu \leq 0.5$) while material is still stable. Materials with different Poisson ratio behave mechanically different [27]. For

pressure-driven solution–diffusion membranes, the surfaces are constrained and compacted while permeated at a given transmembrane pressure (i.e., compressive stress) and feed rate. For perfectly constrained membranes, the transverse strain as results of swelling and compaction is far higher that the longitudinal strain since the membrane is constrained. This leads to membrane densification which results in higher than expected Poisson ratios values. Hence, the Poisson ratios could be very well outside of the normal ranges for membranes in operation.

2.6 Constraint Polymeric Membrane Model

Weber and Newman [28] defined Eqs. 2.9–2.18 in their theoretical study of constraint polymer-electrolyte fuel cells and compared free swelling and constraint swelling polymer membrane (see Fig. 2.6).

For a free swelling membrane;

$$V_f = V_o\left(1 + \frac{\lambda_f \overline{V_o}}{\overline{V_m}}\right) \tag{2.9}$$

For a constraint swelling membrane;

$$V_c = V_o\left(1 + \frac{\lambda_f \overline{V_o}}{\overline{V}_m}(1 - \xi_c)\right) \tag{2.10}$$

where ε_c is the degree of constraint defined by

$$\xi_c = \frac{V_f - V_c}{V_f - V_o} \tag{2.11}$$

where V_o, V_f, and V_c are the initial dry membrane volume, free swollen membrane volume, and the constraint swollen membrane volume, respectively. λ_f, $\overline{V_m}$, $\overline{V_o}$ and ξ_c are the unknown average membrane solvent content, partial molar volume of the membrane and solvent, and the degree of constraint of a free swelling membrane, respectively.

For a membrane undergoing free and constraint swelling, Weber and Newman [28] defined the chemical potential internal and external of the membrane to be equal at equilibrium in Eqs. 2.12–2.14.

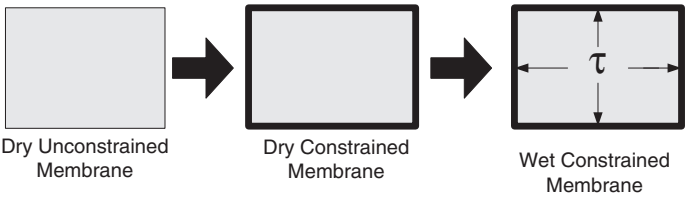

Fig. 2.6 Membrane undergoing constrain swelling [28]

$$\mu_{\mathrm{f,c}}^{\mathrm{int}} = \mu_{\mathrm{f,c}}^{\mathrm{ext}} \tag{2.12}$$

$$\mu_{\mathrm{f}} = \mu^{*} + RT \ln \lambda_{\mathrm{f}} EW + 2RT \sum_{j=1}^{n} \chi_{i,j}^{*} M_j \tag{2.13}$$

$$\mu_{\mathrm{c}} = \mu^{*} + RT \ln \lambda_{\mathrm{c}} EW + 2RT \sum_{j=1}^{n} \chi_{i,j}^{*} M_j + \overline{V_{\mathrm{o}}}\tau \tag{2.14}$$

$$\mu_{\mathrm{f}} = \mu_{\mathrm{c}} \tag{2.15}$$

$$\tau = \frac{RT}{\overline{V_{\mathrm{o}}}} \ln\left(\frac{\lambda_{\mathrm{c}}}{\lambda_{\mathrm{f}}}\right) \tag{2.16}$$

$$\tau = -K \ln\left(\frac{V_{\mathrm{c}}}{V_{\mathrm{f}}}\right) \tag{2.17}$$

$$\left(\frac{\lambda_{\mathrm{c}}}{\lambda_{\mathrm{f}}}\right) = \left(\frac{\overline{V_{\mathrm{m}}} + \overline{V_{\mathrm{o}}}(1 - \xi_{\mathrm{c}})\lambda_{\mathrm{f}}}{\overline{V_{\mathrm{m}}} + \overline{V_{\mathrm{o}}}\lambda_{\mathrm{f}}}\right)^{\frac{K\overline{V_{\mathrm{o}}}}{RT}} \tag{2.18}$$

where $\mu_{\mathrm{fc}}^{\mathrm{int}}$ and $\mu_{\mathrm{fc}}^{\mathrm{ext}}$ are the chemical potential for free (f) and constraint (c) relative to the internal and external of the membrane. μ^{*} is the reference chemical potential. EW, M_{j}, K, and τ are the equivalent membrane weight; molality of the solute j in the membrane, K is the bulk modulus and dilatation stress, respectively. R and T are the molar gas constant and the temperature, respectively.

References

1. Ceresana Market Intelligence Consulting, (2014). Market Stud: Solvents (3rd ed.). http://www.ceresana.com/en/market-studies/chemicals/solvents/
2. Anim-Mensah, A. R. (2007). Evaluation of solvent resistant nanofiltration (SRNF) membranes for small-molecule purification and recovery of polar aprotic solvents for re-use (Ph.D. thesis, University of Cincinnati, OH, 2007).
3. Lowery, T. H., & Richardson, K. S. (1987). *Mechanism and theory in organic chemistry* (3rd ed.). San Francisco: Benjamin-Cummings Publishing Company.
4. Barto, A. F. M. (1991). *CRC handbook of solubility parameters and other cohesion parameters* (2nd ed.). Boca Raton: CRC Press LLC.
5. Hansen, C. M. (2007). *Hansen solubility parameters: A user's handbook*. Boca Raton: CRC Press LLC.
6. Anim-Mensah, A. R. (2012). *Nanofiltration membranes assessment for organic systems separations*. Germany: LAP LAMBERT Academic Publishing.
7. Anim-Mensah, A. R., Krantz, W. B., & Govind, R. (2008). Studies on polymeric nanofiltration-based water softening and the effects of anion properties on the softening process. *European Polymer Journal, 44*, 2244–2252.

8. Gupta, V. K., Hwang, S. T., Krantz, W. B., & Greenberg, A. R. (2007). Characterization of nanofiltration and reverse osmosis membrane performance for aqueous salt solutions using irreversible thermodynamics. *Desalination, 208*, 1–18.
9. Koros, W. J., Ma, Y. H., & Shimidzu, T. (1996). Terminology for membranes and membranes processes. *Journal of Membrane Science, 120*, 149–159.
10. Hicke, H. G., Lehmann, I., Malsch, G., Ulbricht, M., & Becker, M. (2002). Preparation and characterization of a novel solvent-resistant and autoclavable polymer membrane. *Journal of Membrane Science, 198*, 187–196.
11. Persson, K. M., Gekas, V., & Trägårdh, G. (1995). Study of membrane compaction and its influence on ultrafiltration water permeability. *Journal of Membrane Science, 100*, 155–162.
12. Tarnawski, V. R., & Jelen, P. (1986). Estimation of compaction and fouling effects during membrane processing of cottage cheese whey. *Journal of Food Engineering, 5*, 75–90.
13. Anim-Mensah, A. R., Franklin, J. E., Palsule, A. S., Salazar, L. A., & Widenhouse, C. W. (2010). Characterization of a biomedical grade silica-filled silicone elastomer using ultrasound, advances in silicones and silicone-modified materials. *ACS Symposium Series, 1051*, 85–98. (Chap. 8).
14. Gardner, S. H. (1998). An investigation of the structure-property relationships for high performance thermoplastic matrix, carbon fiber composites with a tailored polyimide interphase (Ph.D. dissertation, Virginia Polytechnic Institute and State University, 1998).
15. Harris, B. (1999). *Engineering composite materials*. London: The Institute of Materials.
16. Patel, M. C., & Shah, A. D. (2002). Poly(amides–imides) based on amino end-capped polyoligomides. *Oriental Journal of Chemistry, 1*, 19.
17. Charlier, C. (2012). *Study of materials, polymer data*. HELMo-Gramme Institute Belgium. Retrieved August 6, 2012, from http://www.gramme.be/unite4/Study%20of%20Materials/Polymers%20Annex.pdf.
18. Mark, J. E. (1999). *Polymer data handbook* (3rd ed.). Oxford: Oxford University Press Inc.
19. Dupont Kapton Polyimide Film General Specifications, Bulletin GS-96-7. Retrieved August 6, 2012, from http://www.dupont.com/kapton/general/H-38479-4.pdf.
20. Stafie, N. (2004). Poly(dimethylsiloxane)-based composite nanofiltration membranes for non-aqueous applications (Ph.D. dissertation, University of Twente, The Netherlands, 2004).
21. Technical Data, Solvay Specialty Polymer. Retrieved August 6, 2012, from http://www.solvayplastics.com/sites/solvayplastics/EN/specialty_polymers/Pages/solvay-specialty-polymers.aspx.
22. Burke, J. (1984). *Solubility parameter: Theory and application* (Vol. 3, 13–58). AIC Book and Paper Group Annual.
23. Matweb, Material Property Data. Retrieved August 6, 2012, from www.matweb.com.
24. Strong, A. B. (2008). *Fundamental of composite manufacturing materials, methods and applications* (2nd ed.). Dearborn: Society of Manufacturing Engineering.
25. Wang, Z. (2011). Polydimethylsiloxane mechanical properties measured by macroscopic compression and nanoindentation techniques (Ph.D. thesis, University of South Florida, 2011).
26. Fung, Y. C. (1968). *Foundation of solid mechanics*. Englewood, NJ: Prentice-Hall.
27. Greaves, G. N., Greer, A. L., Lakes, R. S., & Rouxel, T. (2011). Poisson's ratio and modern materials. *Nature Materials, 10*, 823–837.
28. Weber, A. Z., & Newman, J. (2004). A theoretical study of membrane constraint in polymer-electrolyte fuel cells materials, Interfaces, and electrochemical phenomena. *AIChE Journal, 50*, 3215–3226.

http://www.springer.com/978-3-319-12408-7

Prediction of Polymeric Membrane Separation and Purification Performances

A Combined Mechanical, Chemical and Thermodynamic Model for Organic Systems

Anim-Mensah, A.; Govind, R.

2015, XVIII, 51 p. 30 illus., 22 illus. in color., Softcover
ISBN: 978-3-319-12408-7